BI-TP 2000/41

Quark Mass and Flavour Dependence of the QCD Phase Transition

F. Karsch, E. Laermann and A. Peikert

Fakultät für Physik, Universität Bielefeld, D-33615 Bielefeld, Germany

ABSTRACT

We analyze the quark mass and flavour dependence of the QCD phase transition temperature. When the lightest pseudo-scalar meson mass ($m_{\rm PS}$) is larger than 2 GeV the critical temperature is controlled by the gluonic sector of QCD alone. For smaller values of the lightest meson mass the pseudo-critical temperature decreases slowly with $m_{\rm PS}$. For a large regime of meson masses the pseudo-critical temperature of 2-flavour QCD is about 10% larger than in the 3-flavour case. On lattices with temporal extent $N_\tau = 4$ an extrapolation to the chiral limit yields $T_c = (173\pm8)$ MeV and (154 ± 8) MeV for 2 and 3-flavour QCD, respectively. We also analyze dynamical quark mass effects on the screening of the heavy quark potential. A detailed analysis of the heavy quark free energy in 3-flavour QCD shows that close to T_c screening effects are approximately quark mass independent already for pseudo-scalar meson masses $m_{\rm PS} \lesssim 800$ MeV and screening sets in at distances $r \simeq 0.3$ fm.

December 2000

1 Introduction

One of the most prominent non-perturbative features of QCD is the existence of a chiral symmetry restoring and deconfining phase transition at high temperature. Details of this phase transition, the quantitative value of the transition temperature as well as the order of the transition, will depend on basic parameters of QCD, *i.e.* the number of flavours (n_F) and the values of the quark masses (m_q). The influence of global symmetries of the QCD Lagrangian on the order of the phase transition is well understood and predictions in the chiral [1] as well as quenched [2] limit have to a large extent been verified by lattice calculations. It has been shown that the chiral transition is first order in 3-flavour QCD [3] and likely to be continuous in the 2-flavour case [4]. The explicit flavour as well as quark mass dependence of the transition temperature itself, however, is not related to universal properties and therefore is less well understood.

Of great interest is, of course, a quantitative determination of the QCD transition temperature[a] in the limit of light quark masses. The transition temperatures in 2 and 3-flavour QCD will provide upper and lower limits for the transition temperature of QCD with two light and a heavier strange quark mass. Previous calculations of the transition temperature in QCD with dynamical quarks have shown that it is significantly smaller than the critical temperature determined for the deconfinement transition which occurs in the limit of infinitely heavy quarks, *i.e.* in the SU(3) gauge theory [5]. The quark mass dependence of the QCD transition temperature, however, is not well understood. In particular, we would like to understand in more detail what sets the scale for the QCD transition temperature. It is obvious that for large quark masses the valence quark dominated hadronic sector will completely decouple and thermodynamics will be controlled by the gluonic sector alone. In the chiral limit, on the other hand, the light pseudo-scalar mesons are expected to play a dominant role. For instance, studies within the context of $\sigma-$models suggest a strong dependence of the transition temperature on the pseudo-scalar meson mass [6]. For realistic quark mass values the transition temperature itself will be compatible with the value of the pseudo-scalar mass and one may expect that the rich hadronic resonance spectrum will play an important role in this regime [7]. The importance of a rapidly (exponentially) rising resonance mass spectrum for the location of the transition temperature does become apparent already in the $SU(N)$ gauge theories where the transition temperature is rather low ($T_c \simeq 270$ MeV) despite the fact that the lightest excitations in the low temperature phase are glueballs with a mass of about 1.5 GeV [8]. In fact, the value of the phase transition temperature of $SU(N)$ gauge theories can be well understood in terms of the exponentially rising mass spectrum obtained in string models [9]. In order to better understand QCD

[a] In the following we often will talk about the *QCD transition* without distinguishing between a rapid crossover and a true phase transition. This should be clear from the context.

thermodynamics and in particular the critical behaviour close to the transition temperature a detailed analysis of the quark mass dependence of the QCD transition is needed. This problem will be addressed here. In order to be able to discuss the quark mass dependence of the QCD transition temperature we also have to address the question in how far we can compare transition temperatures when the quark masses and/or the number of flavours are varied. We need an appropriate observable to set the scale for the transition temperature which itself is little influenced by these external parameters. In order to reach quantitative conclusions on these questions it will be mandatory to get the intrinsic systematic lattice effects, cut-off dependence and finite volume effects, under control. We therefore will use here improved gauge and fermion actions for our analysis of the quark mass and flavour dependence of the transition temperature in QCD.

We also discuss the influence of dynamical quarks on the heavy quark potential, or more precisely the heavy quark free energy extracted at finite temperature from Polyakov loop correlation functions. In the case of 3-flavour QCD we analyze in detail the quark mass and temperature dependence of the screening of the heavy quark free energy, which becomes significant already below T_c.

This paper is organized as follows. In the next section we will introduce the improved gauge and staggered fermion actions used for our simulations and give some details on the simulation parameters. In Section 3 we present our results on the flavour and quark mass dependence of the transition temperature and give an estimate for the critical temperatures of the chiral transition in massless 2 and 3-flavour QCD. In Section 4 we discuss in more detail the quark mass and temperature dependence of the heavy quark free energy. We finally give our conclusions in Section 5.

2 Thermodynamics with an improved staggered fermion action

The use of improved gauge and fermion actions is mandatory in thermodynamic calculations which generally are performed at quite large values of the lattice spacing, a, because one has to use quite small values for the temporal extent of the lattice. The finite cut-off effects become particularly striking in the calculation of bulk thermodynamic observables. In fact, it has been shown just in these cases that improved actions can be particularly efficient and reduce the cut-off dependence of thermodynamic observables significantly [5].

In the pure gauge sector the tree level, Symanzik improved action yields a satisfactory description of the high temperature ideal gas limit of QCD already on

lattices with temporal extent $N_\tau = 4$ [10]. Similarly good results can be achieved in the fermion sector with improved staggered fermions where three-link terms are added to the ordinary one link discretization of the first order derivatives appearing in the fermion Lagrangian [11, 12].

In the present analysis we will use such an improved action, which in addition to the standard Wilson plaquette term and the standard 1-link staggered fermion action also includes the planar 6-link Wilson loops and bended 3-link terms which improve the rotational symmetry of the staggered fermion action [12]. The partition function for QCD with n_f quark flavours reads

$$Z(T,V) = \int \prod_{x,\mu} \mathrm{d}U_\mu(x) \mathrm{e}^{-\beta S_G} \prod_{q=1}^{n_f} \left(\int \prod_x \mathrm{d}\bar{\chi}_x \mathrm{d}\chi_x \; \mathrm{e}^{-S_F(m_q)} \right)^{1/4} \tag{2.1}$$

where x labels the sites on a hypercubic lattice of size $N_\sigma^3 \times N_\tau$. The gauge (S_G) and fermion (S_F) actions are given by

$$\begin{aligned} S_G &= c_4 \, S_{plaquette} + c_6 \, S_{planar} \\ &\equiv \sum_{x,\nu>\mu} \frac{5}{3} \left(1 - \frac{1}{3} \mathrm{Re\ Tr} \right. \\ &\quad - \frac{1}{6} \left(1 - \frac{1}{6} \mathrm{Re\ Tr} \left(\right. \right. \end{aligned}$$

$$\begin{aligned} S_F(m_q) &= c_1^F S_{1-link,fat}(\omega) + c_3^F S_{3-link} + m_q \sum_x \bar{\chi}_x^f \chi_x^f \\ &\equiv \sum_x \bar{\chi}_x^f \sum_\mu \eta_\mu(x) \left(\frac{3}{8} \left[\right. \right. \end{aligned}$$

$$+ \omega \sum_{\nu \neq \mu}$$

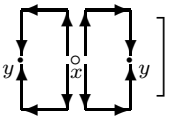

$$\left. \left. + \frac{1}{96} \sum_{\nu \neq \mu} \left[\right. \right. \right.$$

$$\left. \left. \left. \right] \right) \chi_y^f$$

$$+ m_q \sum_x \bar{\chi}_x^f \chi_x^f \quad . \tag{2.3}$$

Here $\eta_\mu(x) \equiv (-1)^{x_0 + .. + x_{\mu-1}}$ denotes the staggered fermion phase factors. Furthermore, we have made explicit the dependence of the fermion action on different quark

flavours q, and the corresponding bare quark masses m_q, and give an intuitive graphical representation of the action. The tree level coefficients c_1^F and c_3^F appearing in S_F have been fixed by demanding rotational invariance of the free quark propagator at $\mathcal{O}(p^4)$ ("p4-action") [11]. In addition the 1-link term of the fermion action has been modified by introducing "fat" links [13] with a weight $\omega = 0.2$. The use of fat links does lead to a reduction of the flavour symmetry breaking close to T_c and at the same time does not modify the good features of the p4-action at high temperature, *i.e.* it has little influence on the cut-off dependence of bulk thermodynamic observables in the high temperature phase [11, 12]. Further details on the definition of the action are given in [11].

For simplicity, in the following we will refer to the p4-action with a fat 1-link term combined with the tree level improved gauge action as *the p4-action*.

Numerical simulations with dynamical fermions have been performed using the Hybrid R algorithm [14]. This algorithm introduces systematic errors which depend quadratically on the step size $\delta\tau$ used for the integration of molecular dynamics trajectories. We have verified on a small $8^3 \times 4$ lattice that the systematic errors with our improved action are similar in magnitude to those found for the standard action [15]. In our simulations we use a step size $\delta\tau = \min\{0.4\, m_q, 0.1\}$. The length of the molecular dynamics trajectories has been chosen to be $\tau = 0.8$.

3 Critical Temperature in 2, 2+1 and 3 Flavour QCD

In this section we want to discuss our results for the pseudo-critical temperatures obtained for 2 and 3-flavour QCD with different quark masses. In addition to the results obtained with identical quark mass values for all flavours we also will present the result of a calculation for (2+1)-flavour QCD, *i.e.* for QCD with two light quark flavours ($m_{u,d} = 0.1$) and one heavier flavour ($m_s = 0.25$). Of course, these bare quark mass parameters receive a multiplicative renormalization. For an easier comparison with the better known parameters of the unimproved staggered fermion action we note that the bare quark parameter, m_q, of the p4-action corresponds to about twice the bare quark mass in the unimproved staggered action.

The calculations with degenerate quark masses cover a range of pseudo-scalar meson mass from about 250 MeV up to the quenched limit of infinitely heavy mesons. We will analyze the quark mass dependence of the pseudo-critical temperature and discuss its extrapolation to the chiral limit. This involves two steps: First of all one has to determine the pseudo-critical couplings, $\beta_c(m_q)$, on finite temperature lattices of size $N_\sigma^3 \times N_\tau$. One then has to calculate physical observables at zero temperature

$n_f = 2$				
$m_{u,d}$	$N_\sigma^3 \times N_\tau$	$\#\beta$	#iter.	β_c
0.025	$8^3 \times 4$	3	3200	3.542 (7)
0.05	$8^3 \times 4$	4	3700	3.585 (11)
0.10	$16^3 \times 4$	10	36300	3.646 (4)
0.20	$8^3 \times 4$	6	6300	3.778 (12)
$n_f = 2+1$				
$m_{u,d}/m_s$	$N_\sigma^3 \times N_\tau$	$\#\beta$	#iter.	β_c
0.10/0.25	$16^3 \times 4$	10	31550	3.543 (2)

Table 1: Simulation parameters for the determination of the critical temperature for 2 and $2+1$ flavours. The largest lattice size simulated, the number of β values and iterations as well as the finally determined pseudo-critical couplings are given.

which allow to extract the lattice spacing at $\beta_c(m_q)$ through which the temperature is fixed, $T_c = 1/N_\tau a(\beta_c)$.

3.1 Critical couplings on $16^3 \times 4$ lattices

The finite temperature calculations have been performed on lattices with temporal extent $N_\tau = 4$ and spatial lattice sizes $N_\sigma = 8$, 12 and 16. For each value of the quark mass we have performed simulations at several values of the gauge coupling β. Details on the simulation parameters and the statistics collected on our largest lattices are given in Table 1. For the determination of the pseudo-critical couplings we calculated the average Polyakov loop,

$$L \equiv \frac{1}{N_\sigma^3} \left| \sum_{\vec{x}} L(\vec{x}) \right| = \frac{1}{N_\sigma^3} \left| \frac{1}{3} \sum_{\vec{x}} \mathrm{Tr} \prod_{x_4=1}^{N_\tau} U_4(\vec{x}, x_4) \right| \quad , \tag{3.1}$$

and used a noisy estimator for the chiral condensate which is based on 25 random vectors R_i,

$$\overline{\psi}\psi = \frac{1}{N_\tau N_\sigma^3} \frac{n_f}{4} \mathrm{Tr}\ M^{-1} \simeq \frac{n_f}{100 N_\tau N_\sigma^3} \sum_{i=1}^{25} R_i^\dagger M^{-1} R_i \quad . \tag{3.2}$$

As usual we have introduced here the fermion matrix M, which is defined through the matrix form of Eq. 2.3, *i.e.* $S_F \equiv \sum_{q=1}^{n_f} \bar{\chi}\ M(m_q)\ \chi$. At each value of the quark

mass the data from runs at all β-values have been used in a Ferrenberg-Swendsen reweighting [16] to determine the maxima in the related Polyakov-loop and chiral susceptibilities[b],

$$\begin{aligned} \chi_L &\equiv N_\sigma^3 \left(\left\langle L^2 \right\rangle - \langle L \rangle^2 \right) \quad , \\ \chi_{\overline{\psi}\psi,\mathrm{disc}} &= \frac{1}{N_\tau N_\sigma^3} \frac{n_f}{16} \left(\left\langle \left(\mathrm{Tr}\ M^{-1} \right)^2 \right\rangle - \left\langle \mathrm{Tr}\ M^{-1} \right\rangle^2 \right) \end{aligned} \tag{3.3}$$

as well as the susceptibility of the gauge action,

$$\chi_S \equiv N_\sigma^3 N_\tau \left(\left\langle S_G^2 \right\rangle - \langle S_G \rangle^2 \right) \quad . \tag{3.4}$$

At intermediate values of the quark mass the transition to the high temperature phase of QCD is not related to any form of critical behaviour in thermodynamic observables. Nonetheless, the maxima of the susceptibilities define pseudo-critical couplings, $\beta_c(m_q)$, for the transition to the high temperature phase of QCD, which manifests itself in a sudden change of thermodynamic observables in a small temperature interval[c]. For small (vanishing) and large values of the quark mass the transition, however, becomes a true phase transition in the infinite volume limit. In these cases the pseudo-critical couplings give finite volume estimates for the location of the critical point in the thermodynamic limit.

Previous analyses of the volume dependence of the pseudo-critical couplings performed with unimproved gauge and staggered fermion actions [4, 15] have shown that finite size effects are small at intermediate values of the quark mass. Moreover, the pseudo-critical couplings seem to show little dependence on the observable used to define them. This is also supported by our analysis of finite volume effects in simulations with the p4-action. In the case of 3-flavour QCD we have determined the pseudo-critical couplings $\beta_c(m_q)$ for 10 different values of the bare quark mass in the interval $0.01 \leq m_q \leq 1.0$ on lattices of spatial extent $N_\sigma = 8$, 12 and 16. The results of this analysis are summarized in Table 2. Within the statistical errors of the present analysis we do not observe any clear volume dependence at intermediate values of the quark mass and even not for the smallest value, $m_q = 0.01$, considered here. This, however, is no longer true for large masses, where the onset of the first order deconfining transition leads to large correlation lengths. This is reflected in a strong volume dependence of the peak height of the susceptibilities and a visible volume dependence of the pseudo-critical couplings. Note that the location of the

[b] Note that we only calculate the disconnected part of the complete chiral susceptibility, $\chi_{\overline{\psi}\psi} \sim \partial^2 \ln Z / \partial (m_q)^2$.

[c] It recently has been suggested that the sudden change in behaviour at a certain pseudo-critical temperature may be characterized in terms of a non-thermal, percolation phase transition [17].

				pseudo critical couplings β_c		
m_q	N_σ	# β	# iter.	max(χ_S)	max(χ_L)	max($\chi_{\bar{\psi}\psi,disc}$)
0.01	8	9	10300	3.2865 (98)	3.2887 (65)	3.2841 (57)
	16	3	4440	3.2784 (89)	3.2804 (37)	3.2806 (20)
0.025	8	8	14000	3.3265 (93)	3.3318 (24)	3.3281 (25)
	16	6	8200	-	3.3428 (159)	3.3194 (21)
0.05	8	11	16250	-	3.4018 (35)	3.3930 (201)
	16	4	4500	3.3866 (47)	3.3950 (150)	3.3877 (26)
0.10	8	12	25100	3.4637 (34)	3.4864 (25)	3.4842 (151)
	16	9	15350	3.4752 (10)	3.4856 (138)	3.4756 (14)
0.20	8	16	39250	3.5184 (462)	3.6216 (27)	3.6204 (32)
	12	5	18700	3.5986 (25)	3.6020 (32)	3.6004 (18)
	16	8	29650	3.5998 (14)	3.6017 (17)	3.6000 (33)
0.40	8	11	36600	3.7756 (64)	3.7848 (23)	3.7808 (27)
	12	3	11700	3.7810 (24)	3.7781 (17)	3.7797 (16)
	16	5	16250	3.7653 (16)	3.7719 (33)	3.7746 (40)
0.60	8	12	33100	3.7983 (159)	3.8865 (17)	3.8806 (12)
	12	4	16500	3.8718 (47)	3.8770 (16)	3.8798 (38)
	16	6	41750	3.8210 (233)	3.8766 (6)	3.8764 (6)
0.70	16	4	24000	3.7983 (159)	3.8865 (17)	3.8806 (12)
0.80	16	3	25300	3.9358 (18)	3.9377 (10)	3.9368 (14)
1.00	8	8	21750	3.9680 (6)	3.9686 (27)	3.9663 (11)
	12	5	24520	3.9717 (39)	3.9712 (22)	3.9711 (15)
	16	8	101300	3.9771 (15)	3.9778 (10)	3.9808 (16)
∞	8	10	129000	4.0554 (27)	4.0745 (17)	-
	12	14	154900	4.0708 (27)	4.0708 (6)	-
	16	8	157500	4.0719 (7)	4.0715 (5)	-
	24	3	75200	4.0724 (4)	4.0722 (4)	-
	32	1	46800	4.0733 (4)	4.0729 (3)	-
	∞	-	-	4.0732 (4)	4.0730 (3)	-

Table 2: Pseudo-critical couplings of the p4-action calculated on lattices with spatial extent $N_\sigma = 8$, 12 and 16 and temporal extent $N_\tau = 4$ for 3-flavour QCD with different quark masses. Errors on the maxima of the susceptibilities have been determined from a jackknife analysis.

peak of the action susceptibility χ_S shows the strongest volume dependence. However, on the largest lattice ($16^3 \times 4$) it also agrees within statistical errors with all the other observables used to locate the pseudo-critical points. In particular, we do not find any systematic volume dependence in the peak location of χ_L and $\chi_{\bar{\psi}\psi,\mathrm{disc}}$ for quark masses $m_q \leq 0.6$. The pseudo-critical couplings taken from the largest lattice which have been used for the determination of the critical temperature are also given in Table 1.

The extrapolation of the pseudo-critical couplings to the chiral limit will depend on the order of the phase transition which, in accordance with present knowledge from lattice calculations, is expected to be second order for $n_f = 2$ and first order for $n_f \geq 3$ [1]. If the transition is first order in the chiral limit it will remain to be first order also for small values of the quark mass. The shift in the critical coupling will then depend linearly on the quark mass with a slope controlled by the zero quark mass discontinuities in the order parameter and gauge action. From a Taylor expansion of the free energy below and above the critical point one obtains[d],

$$\beta_c(m_q) = \beta_c(0) + \frac{\Delta\langle\bar{\psi}\psi\rangle}{\Delta\langle S_G\rangle} m_q \qquad , \qquad n_f \geq 3 \quad . \tag{3.5}$$

In the case of a second order transition, however, the diverging correlation length at the critical point will lead to a stronger variation of the critical couplings with the quark mass. From the non-analytic structure of the singular part of the free energy one finds that the critical couplings will scale like,

$$\beta_c(m_q) = \beta_c(0) + c \cdot (m_q)^{1/\beta\delta} \qquad , \qquad n_f = 2 \quad . \tag{3.6}$$

Here $1/\beta\delta$ is a combination of critical exponents which for the case of 2-flavour QCD are expected to be those of the three dimensional $O(4)$ symmetric spin models, *i.e.* in the continuum limit one expects to find $1/\beta\delta \simeq 0.55$. Of course, the regular part of the free energy will also add a linear dependence on m_q to this leading order behaviour.

In Figure 1 we show our results for $\beta_c(m_q)$ in 2 and 3-flavour QCD obtained for small and intermediate values of the quark mass with the p4-action. Furthermore, we show results from calculations with the standard Wilson gauge and standard staggered fermion action [15, 19, 20, 21, 22]

The similarity in the quark mass dependence of $\beta_c(m_q)$ seen in Figure 1 for the 2 and 3-flavour cases suggests that for n_f=2 also the subleading corrections, linear

[d]This follows the same line of arguments given in Ref. [18] for the quark mass dependence of the deconfinement transition in the limit of heavy quarks.

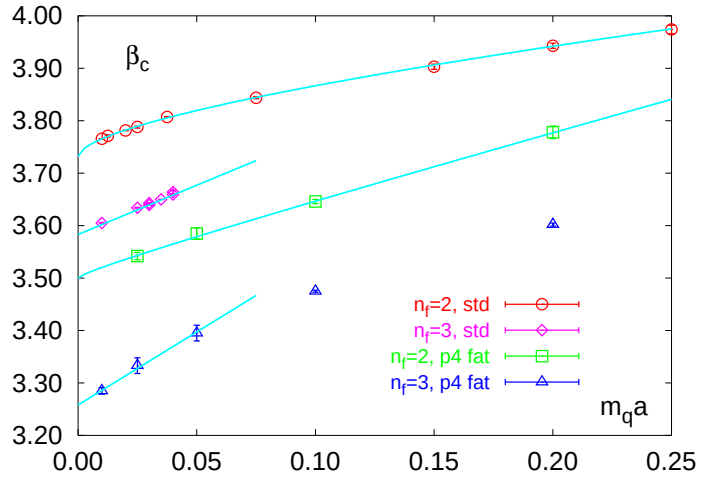

Figure 1: Pseudo-critical couplings of 2 and 3 flavour QCD versus bare quark mass calculated on lattices of size $16^3 \times 4$ with the standard Wilson plaquette and standard staggered fermion action (std) and the improved gauge and fermion action (p4) described in section 2. The data for the standard action have been shifted by $\Delta\beta = -1.5$. Lines show linear fits to the 3-flavour data for $m_q \leq 0.05$ and "O(4)+linear" fits for the 2-flavour data with $m_q \leq 0.2$.

in m_q are still important in the quark mass regime explored by present simulations. We thus have extrapolated the critical couplings to the chiral limit by assuming the $O(4)$ symmetric ansatz given in Eq. 3.6 and allowing for a subleading term linear in m_q. This yields for

$\underline{n_f = 2}$:

$$\beta_c(0) = \begin{cases} 5.232 \pm 0.002 & \text{standard gauge and fermion action} \\ 3.48 \pm 0.03 & \text{improved gauge and fermion action} \end{cases} \tag{3.7}$$

The result for the standard staggered action is consistent with fits solely based on the ansatz given in Eq. 3.6 with free exponent $1/\beta\delta$ [15, 23] as well as fits in which the exponent has been fixed to its $O(4)$ value, *i.e.* $1/\beta\delta = 0.55$.

In the 3-flavour case, on the other hand, the linear dependence on m_q is evident for small quark masses and linear fits with a small $\chi^2/(d.o.f.)$ can be performed for $m_q \leq 0.05$. From these fits we find for the critical couplings of the 3-flavour theory in the chiral limit,

$\underline{n_f = 3:}$

$$\beta_c(0) = \begin{cases} 5.083 \pm 0.004 & \text{standard gauge and fermion action} \\ 3.258 \pm 0.004 & \text{improved gauge and fermion action} \end{cases} \tag{3.8}$$

The quark mass dependence of $\beta_c(m_q)$ is significantly different in the case of improved and unimproved actions. From the fits of the critical couplings we find,

$$\frac{\Delta\langle\bar{\psi}\psi\rangle}{\Delta\langle S_G\rangle \cdot N_\tau} = \begin{cases} 0.49 \pm 0.01 & \text{standard action} \\ 0.70 \pm 0.04 & \text{improved action} \end{cases} \tag{3.9}$$

However, in order to relate these slope parameters to a physical observable, the ratio of the discontinuity in the chiral condensate and the latent heat $\Delta\epsilon$, on still has to determine a normalization constant $Z_m(\beta_c)$ [24] that turns $\langle\bar{\psi}\psi\rangle$ into a renormalization group invariant observable,

$$\frac{T_c \cdot \Delta(\bar{\psi}\psi)^{RGI}}{\Delta\epsilon} = \frac{\Delta\langle\bar{\psi}\psi\rangle}{\Delta\langle S_G\rangle \cdot N_\tau} Z_m^{-1}(\beta_c) \quad . \tag{3.10}$$

This may partly account for the observed difference between the standard and improved actions.

3.2 Setting the scale at zero temperature

In order to relate the pseudo-critical couplings to physical temperatures and to perform the extrapolation to the chiral limit we have performed zero temperature simulations on lattices of size 16^4. In addition to pseudo-scalar ($m_{\rm PS}$) and vector (m_V) meson masses we also have calculated the string tension (σ) from large Wilson loops.

The spectrum calculations performed at $\beta_c(m_q)$ follow the conventional approach. They are based on wall source operators as described e.g. in Ref. [25]. Masses have then been extracted from the exponential decay of correlation functions constructed from wall source and local sink operators. Also the calculation of the string tension is based on a standard approach. We use smeared Wilson loops [26] from which we extract a potential which then is fitted to an ansatz which includes a Coulomb and a linearly rising term. The notion of a string tension in the presence of dynamical quarks does, however, require a bit more explanation. In the presence of dynamical quarks the heavy quark potential is no longer linear at large distances as the spontaneous creation of quark anti-quark pairs from the vacuum will lead to string breaking. Nonetheless, it has been found that the "potential" extracted from Wilson

loops does not show evidence for string breaking[e] even at distances of up to about 2fm [27]. Wilson loops thus can still be used to extract a "string tension" from its large distance behaviour. As will become clear in the following a comparison with quenched and partially quenched spectrum calculations shows that this string tension shows only little quark mass and flavour dependence.

The meson masses and the string tension calculated at $\beta_c(m_q)$ for 2 and 3-flavour QCD are given in Table 3. Here we also give the result from a simulation of (2+1)-flavour QCD. Furthermore, for $n_f = 3$ we have performed calculations with bare quark mass $m_q = 0.1$ at various β-values that cover the region of critical couplings obtained with small quark masses. We will use these data in the next section to determine the vector meson mass (m_ρ) in the chiral limit at $\beta_c(m_q = 0)$.

In order to quantify the flavour and quark mass dependence of the QCD transition temperature it is, of course, important to understand to what extent the zero temperature observables used to set the scale are dependent on m_q and n_f. Clearly the hadron masses will depend on the bare quark masses m_q. With decreasing quark masses one also might expect some n_f-dependence resulting from sea quark contributions to the hadron masses. Quenched spectrum calculations, however, suggest that the latter effect is small compared to the explicit valence quark mass dependence [29]. The string tension, on the other hand, is expected to show a much weaker dependence on the quark masses. This is supported by the fact that in the quenched limit, *i.e.* in the pure $SU(3)$ gauge theory the value for the string tension deduced from the ratio $(\sqrt{\sigma}/m_\rho)_{\rm quenched}$ in the limit of vanishing valence quark mass [30] is consistent with phenomenological values used as input in heavy quark spectrum calculations [31].

In Figure 2 we show the ratio $\sqrt{\sigma}/m_{\rm V}$ as a function of $(m_{\rm PS}/m_{\rm V})^2$. In addition to the results obtained from simulations with dynamical quarks at various values of the bare quark mass, we also show in this figure results obtained in quenched QCD [30] and from a partially quenched analysis. For the latter we have performed a spectrum analysis in 3-flavour QCD with valence quarks of mass $m_q = 0.02$ and 0.05 on gauge field configurations generated with dynamical quarks of mass $m_q = 0.1$ at the critical coupling, $\beta_c(m_q = 0.1) = 3.475$. Results for the partially quenched meson masses obtained in this case are given in Table 4. The square root of the string tension in units of the vector meson mass in the limit of vanishing valence quark mass is obtained as

$$\frac{\sqrt{\sigma}}{m_\rho} = \begin{cases} 0.552 \pm 0.013 & \text{, quenched [30]} \\ 0.532 \pm 0.018 & \text{, partially quenched for } m_q = 0.1,\ n_f = 3 \end{cases} \tag{3.11}$$

[e]String breaking has been found to occur at non-zero temperature where the heavy quark free energy can be extracted from Polyakov loop correlation functions [28]. We will discuss this in more detail in Section 4.

$N_f = 2$						
$m_{u,d}$	β_c	σa^2	$m_{\rm PS} a$	$m_{\rm V} a$	$T_c/\sqrt{\sigma}$	$T_c/m_{\rm V}$
0.025	3.542 (7)	0.300 (15)	0.507 (2)	1.175 (35)	0.456 (11)	0.213 (6)
0.05	3.585 (11)	0.286 (14)	0.697 (6)	1.260 (35)	0.467 (11)	0.198 (6)
0.10	3.646 (4)	0.271 (10)	0.958 (2)	1.377 (25)	0.480 (10)	0.182 (4)
0.20	3.778 (12)	0.205 (12)	1.295 (15)	1.530 (35)	0.552 (16)	0.163 (4))
$N_f = 2+1$						
$m_{u,d}/m_s$	β_c	σa^2	$m_{\rm PS} a$	$m_{\rm V} a$	$T_c/\sqrt{\sigma}$	$T_c/m_{\rm V}$
0.10/0.25	3.543 (2)	0.271 (11)	0.962 (3)	1.343 (20)	0.480 (10)	0.186 (3)
$N_f = 3$						
$m_{u,d}$	β_c	σa^2	$m_{\rm PS} a$	$m_{\rm V} a$	$T_c/\sqrt{\sigma}$	$T_c/m_{\rm V}$
0.025	3.329 (15)	0.350 (20)	0.509 (1)	1.290 (40)	0.423 (12)	0.194 (10)
0.05	3.395 (15)	0.303 (13)	0.706 (6)	1.320 (35)	0.454 (10)	0.189 (6)
0.10	3.475 (2)	0.283 (11)	0.967 (1)	1.415 (15)	0.470 (9)	0.177 (2)
0.20	3.602 (3)	0.248 (4)	1.322 (2)	1.608 (9)	0.502 (4)	0.155 (1)
0.40	3.772 (4)	0.189 (4)	1.814 (4)	1.985 (10)	0.575 (6)	0.126 (1)
0.60	3.877 (2)	0.176 (3)	2.210 (4)	2.347 (12)	0.596 (5)	0.107 (1)
1.00	3.978 (2)	0.154 (2)	2.838 (6)	2.979 (15)	0.637 (4)	0.084 (1)

Table 3: The string tension, pseudo-scalar masses and vector meson calculated at the critical couplings which are given in the second column. In the last two columns we give the critical temperature in terms of the string tension and vector meson mass.

This clearly is also consistent with an extrapolation of the ratio $\sqrt{\sigma}/m_V$ to the chiral limit which yields $\sqrt{\sigma}/m_\rho \simeq 0.50$. Calculated at non-zero values of the bare quark mass this ratio, however, does show a strong dependence on m_q.

We thus find similar results for the ratio $\sqrt{\sigma}/m_\rho$ in the quenched and in the chiral limit. This suggests that the string tension extracted from Wilson loops as well as partially quenched meson masses depend only weakly on the number of flavours and the value of the dynamical quark mass used in a numerical simulation. They thus are suitable observables to set a scale for other physical observables which may be sensitive to these external parameters of QCD.

m_q	$m_{\rm PS}a$	$m_{\rm V}a$
0.02	0.448 (2)	1.08 (1)
0.05	0.695 (2)	1.23 (2)

Table 4: Partially quenched spectrum results in 3-flavour QCD performed at $\beta_c(m_q = 0.1)$ on 16^4 lattices. Results for $m_q = 0.1$ and the corresponding value of the string tension at the critical coupling are given in Table 3.

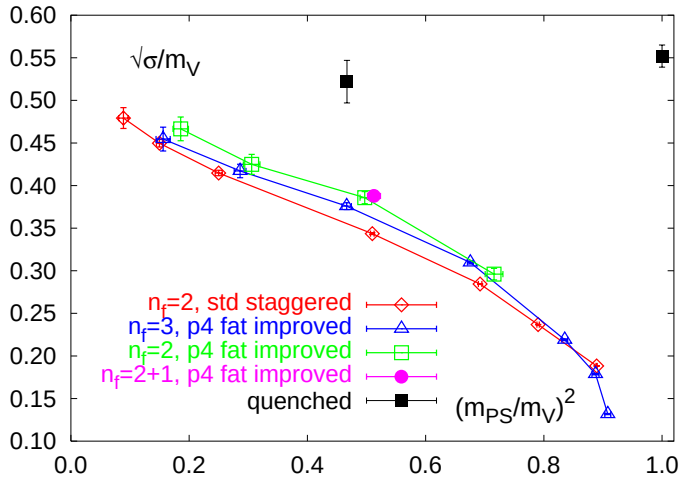

Figure 2: Square root of the string tension in units of the vector meson mass as a function of the ratio of pseudo-scalar and vector meson masses. Shown are results for 2, 2+1 and 3 flavour QCD obtained with the improved gauge and staggered fermion action given in Eqs. 2.2 and 2.3 . Also shown are results from calculations with unimproved staggered fermions [20]. The black squares show results from quenched calculations and partially quenched calculations with a sea quark mass of $m_q = 0.1$.

3.3 Quark mass dependence of the transition temperature

In the previous subsections we have discussed the calculations performed to determine the pseudo-critical couplings for the QCD transition to the high temperature plasma phase and presented zero temperature calculations of meson masses and the string tension which are needed to set the scale for the transition temperature. The resulting pseudo-critical temperatures expressed in units of the square root of the string tension as well as in units of the vector meson mass are given in Table 3 and shown in Figure 3. We note that $T_c/\sqrt{\sigma}$ and $T_c/m_{\rm V}$ show a consistent flavour dependence. The transition temperature decreases slightly when the number of flavours is increased. The effect seems to be somewhat stronger in the latter ratio, which reflects the relative flavour dependence of the two observables used to set

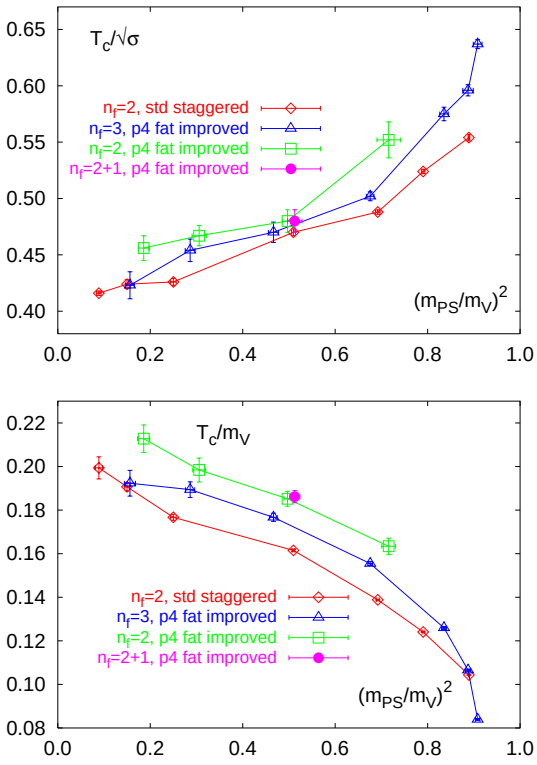

Figure 3: The transition temperature versus $(m_{\rm PS}/m_{\rm V})^2$ for 2 and 3-flavour QCD obtained from calculations with the p4 action on lattices with temporal extent $N_\tau = 4$. Also shown are results from calculations using unimproved gauge and staggered fermion actions [20].

the physical scale (see Figure 2). The quark mass dependence or, correspondingly, the dependence on the meson mass ratio $m_{\rm PS}/m_{\rm V}$, is, however, completely different for $T_c/\sqrt{\sigma}$ and $T_c/m_{\rm V}$. In fact, the decrease of $T_c/m_{\rm V}$ with increasing quark mass mainly reflects the strong quark mass dependence of $m_{\rm V}$ itself and does not represent the physical quark mass dependence of the transition temperature. The ratio $T_c/\sqrt{\sigma}$, on the other hand, shows the expected quark mass dependence; with decreasing quark mass the transition temperature drops from the pure gauge value, $(T_c/\sqrt{\sigma})_{\rm SU(3)} \simeq 0.635$ to a value $(T_c/\sqrt{\sigma})_{\rm chiral} \simeq (0.4 - 0.45)$. This is in accord with the physical picture that with decreasing quark mass hadronic degrees of freedom become lighter and thus get more easily excited in a thermal heat bath. They then can contribute to the overall energy and particle density of the system and thus can trigger the onset of a phase transition already at a lower temperature. Figure 3 thus underlines the importance of a physical observable for setting the scale of T_c which itself is quark mass independent or at least only shows a weak dependence on m_q. Only in this way we can hope to make contact with phenomenological models that discuss the quark mass dependence of T_c. We have argued in the previous subsection that the string tension and partially quenched meson masses fulfill this requirement. We will mainly use here the former observable to set a physically sensible scale for T_c. Of course, an analysis of T_c in units of a hadron masses is still of particular importance in the chiral limit as this provides an experimentally well determined input whereas $\sqrt{\sigma}$ is only indirectly accessible through heavy quark phenomenology.

In Figure 3 we also have shown results for $T_c/\sqrt{\sigma}$ obtained from simulations with unimproved gauge and staggered fermion actions on lattices with temporal extent $N_\tau = 4$. They differ systematically from the results obtained from simulations with improved actions, which indicates that we have to consider the influence of finite cut-off effects on our results. In the case of unimproved staggered fermions simulations of 2-flavour QCD have also been performed on lattices with larger temporal extent, *i.e.* at smaller lattice spacing [34]. These calculations indeed lead to larger values for $T_c/\sqrt{\sigma}$ which are consistent with our results obtained with improved fermions. It thus seems that the simulations with improved gauge and staggered fermion actions lead to a sizeable reduction of cut-off effects.

We have good control over the transition temperatures down to meson mass ratios $m_{PS}/m_V \simeq 0.4$, which corresponds to pion masses of about 370 MeV when one uses the string tension to set a physical scale[f]. The results obtained for $T_c/\sqrt{\sigma}$ in 2 and 3-flavour QCD indicate that the transition temperature is lower in the latter case. From a linear interpolation of our data at intermediate values of the quark

[f]Whenever we use the string tension to convert to physical units we use $\sqrt{\sigma} = 425$ MeV, which is consistent with the quenched and partially quenched results given in Eq. 3.11 and corresponds to $\sqrt{\sigma}/m_\rho = 0.55$.

masses we find

$$\Delta(T_c/\sqrt{\sigma}) \equiv \left(\frac{T_c}{\sqrt{\sigma}}\right)_{n_f=2} - \left(\frac{T_c}{\sqrt{\sigma}}\right)_{n_f=3} \simeq 0.03 \quad \text{for} \quad 0.4 \leq m_{PS}/m_V \leq 0.70 \tag{3.12}$$

Similarly we find $\Delta(T_c/m_V) \simeq 0.015$. This corresponds to a temperature difference of approximately $(10-15)$ MeV.

3.4 Transition temperature in the chiral limit

As pointed out in section 3.1 the pseudo-critical couplings will scale differently close to the chiral limit of 2 and 3-flavour QCD. This, of course, translates into a different scaling of the critical temperatures as a function of the mass of the Goldstone particles,

$$T_c(m_\pi) - T_c(0) \sim \begin{cases} m_q^{1/\beta\delta} \sim m_\pi^{2/\beta\delta} & , n_f = 2 \\ m_q \sim m_\pi^2 & , n_f \geq 3 \end{cases} \quad . \tag{3.13}$$

However, from Figure 3 it is apparent that in the mass regime currently explored by our simulations the dependence of T_c on the Goldstone mass is quite similar for 2 and 3-flavour QCD. As also observed in the analysis of the pseudo-critical couplings discussed in section 3.1 subleading corrections will be of particular importance for the chiral extrapolation in 2-flavour QCD. Subleading contributions linear in m_q will become relevant and will influence the dependence of T_c as well as that of the pseudo-scalar mass on the quark masses. In fact, we find that in a large interval of pseudo-scalar meson masses T_c depends linearly on $m_{\rm PS}$. This is apparent from Figure 4. The line shown there is obtained from a fit to the 3-flavour data in the mass interval, $0.85 < m_{\rm PS}/\sqrt{\sigma} < 5.3$, *i.e.* for 360 MeV $\lesssim m_{\rm PS} \lesssim$ 2.3 GeV. This gave

$$\left(\frac{T_c}{\sqrt{\sigma}}\right)(m_{\rm PS}) = 0.40\ (1) + 0.039\ (4)\ \left(\frac{m_{\rm PS}}{\sqrt{\sigma}}\right) \quad . \tag{3.14}$$

In view of the quite similar functional dependence of T_c on $m_{\rm PS}$ for 2 and 3-flavour QCD it seems that this is not indicative for any form of *chiral behaviour*, although an almost linear dependence of T_c on $m_{\rm PS}$ is just what one would expect to happen in the case of 2-flavour QCD ($2/\beta\delta = 1.1$). We also note the rather weak dependence of T_c on $m_{\rm PS}$. This suggests that the value of T_c is dominantly controlled by a large number of resonances at intermediate mass values which is not so sensitive to modifications of the mass of the lightest states in the spectrum.

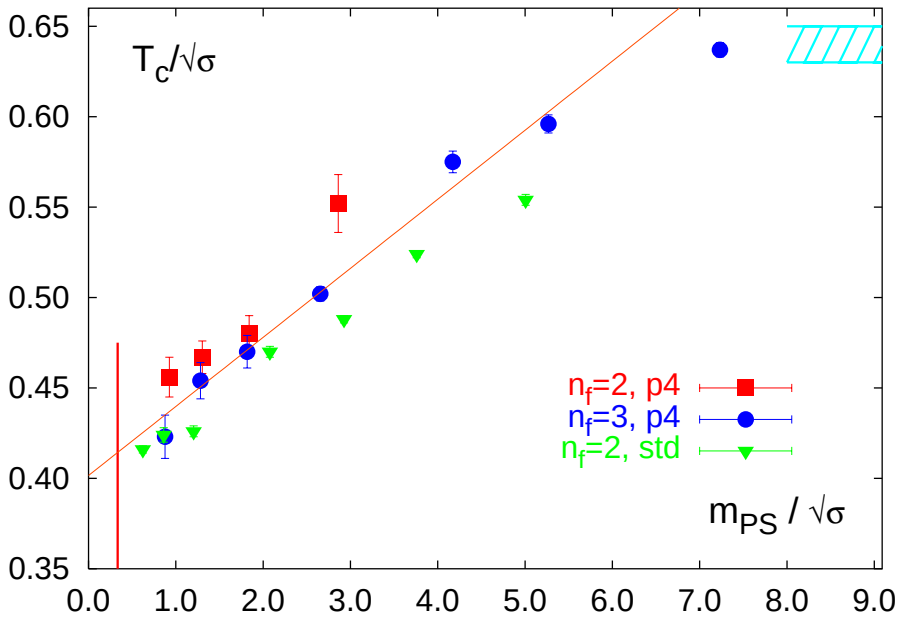

Figure 4: The transition temperature for 2 and 3 flavour QCD in units of the string tension versus $m_{\rm PS}/\sqrt{\sigma}$ obtained with standard (std) [20] and improved (p4) staggered fermions on lattices with temporal extent $N_\tau = 4$. The hatched band to the right of the figure denotes the quenched result, the vertical line to the left is the physical $m_{PS}/\sqrt{\sigma}$ value.

3.4.1 Chiral transition in 3-flavour QCD

In order to get some control over systematic errors resulting from subleading quark mass dependences in the various observables used in our analysis we have performed extrapolations to the chiral limit in different ways:

i) We extrapolate $T_c/\sqrt{\sigma}$ using linear fits in $(m_{PS}/m_V)^2$, $(m_{PS}/\sqrt{\sigma})^2$ and m_q for $m_{PS}/m_V < 0.7$. This yields $T_c/\sqrt{\sigma} = 0.407(15)$, $0.419(15)$ and $0.418(16)$, respectively.

ii) We repeat (i) for T_c/m_V. This yields $T_c/m_\rho = 0.204(5)$, $0.200(3)$ and $0.200(3)$.

iii) We use the vector meson masses calculated at $\beta_c(m_q = 0.05)$ and $\beta_c(m_q = 0.025)$ and extrapolate them to the critical point $\beta_c(m_q \to 0) = 3.258(4)$. This yields $T_c/m_\rho = 0.199(4)$.

We note that (i) yields results consistent with the fit linear in $m_{\rm PS}$ given in Eq.3.14. We also stress that the results obtained from (i) and (ii) imply $\sqrt{\sigma}/m_\rho = 0.49(2)$ for the ratio of the two zero temperature observables used to set the scale. This is consistent with the results shown in Figure 2. The above extrapolations also are consistent with the linear interpolation given in Eq. 3.14 which is shown in Figure 4.

Combining the results of the various fits performed we estimate for the critical temperature of 3-flavour QCD in the chiral limit

$$\frac{T_c}{m_\rho} = 0.20 \pm 0.01 \quad \leftrightarrow \quad T_c = (154 \pm 8)\ \text{MeV} \quad . \tag{3.15}$$

We note that this result has been obtained on lattices with temporal extent $N_\tau = 4$. Although we expect that cut-off effects are small in our calculation with improved gauge and fermion actions a systematic analysis on lattices with larger temporal extent will be needed to perform a controlled extrapolation to the continuum limit. However, we estimate that the systematic error resulting from remaining cut-off effects is of the same size as the statistical error quoted above.

3.4.2 Chiral transition in 2-flavour QCD

As indicated in Eq. 3.13, close to the chiral limit we expect to find a universal scaling behaviour of T_c that is characteristic for the universality class of the second order phase transition. For the quark mass or pion mass values accessible in present computer simulations subleading corrections will, however, still be important. Moreover, the explicit quark mass dependence of the zero temperature observable used to set

the scale has to be taken into account. This is most drastically seen in the ratio T_c/m_V, which decreases with increasing pion mass although one clearly expects that the critical temperature in physical units increases with increasing mass of the lightest particles in the heat bath. This is correctly reflected in the ratio $T_c/\sqrt{\sigma}$. In the entire quark mass regime analyzed so far the quark mass dependence of the ratio T_c/m_V, however, is dominated by the explicit quark mass dependence of m_V. An appropriate ansatz for the quark mass dependence of T_c/m_V is

$$\left(\frac{T_c}{m_V}\right)(m_q) = \left(\frac{T_c}{m_V}\right)(0) + a\, m_q^{1/\beta\delta} + b\, m_q \quad , \tag{3.16}$$

where one should find $a > 0$ and $b < 0$. Thus, also this ratio will ultimately approach the chiral limit from above. With the presently used quark masses, however, the subleading term, linear in m_q, apparently still gives the dominant contribution. For 2-flavour QCD the ratio T_c/m_V thus clearly does not yet reflect the expected leading order quark mass dependence of T_c.

In performing the extrapolation to the chiral limit we followed the strategy outlined in the previous section. For the case of the ratio $T_c/\sqrt{\sigma}$ we have performed extrapolations linear in m_q as well as assuming the $O(4)$ universal behaviour $\sim m_q^{0.55}$. In the case of T_c/m_V, however, we only use the linear extrapolation. From this we find

$$\frac{T_c}{m_\rho} = 0.225 \pm 0.010 \quad , \quad \frac{T_c}{\sqrt{\sigma}} = 0.425 \pm 0.015 \tag{3.17}$$

We note again that this implies for the ratio of the two observables used to set the scale, $\sqrt{\sigma}/m_\rho = 0.53(3)$. Using the rho meson mass to convert the critical temperature to physical units we find

$$T_c = (173 \pm 8)\ \text{MeV} \quad . \tag{3.18}$$

This result is consistent with earlier estimates obtained from calculations with the standard staggered fermion action [5] and also with a recent calculation performed with clover improved Wilson fermions and a renormalization group improved gauge action [32]. We stress again that the errors quoted above are statistical only. Similar to the $n_f = 3$ case we expect that systematic errors are of similar size.

Let us finally comment on the critical temperature in the physically most interesting case of (2+1)-flavour QCD. The simulations performed in this case still use too heavy quarks in the light quark sector, *i.e.* $m_{u,d} = 0.1$. However, even in this case we find that the pseudo-critical temperature is closer to that of 2-flavour QCD

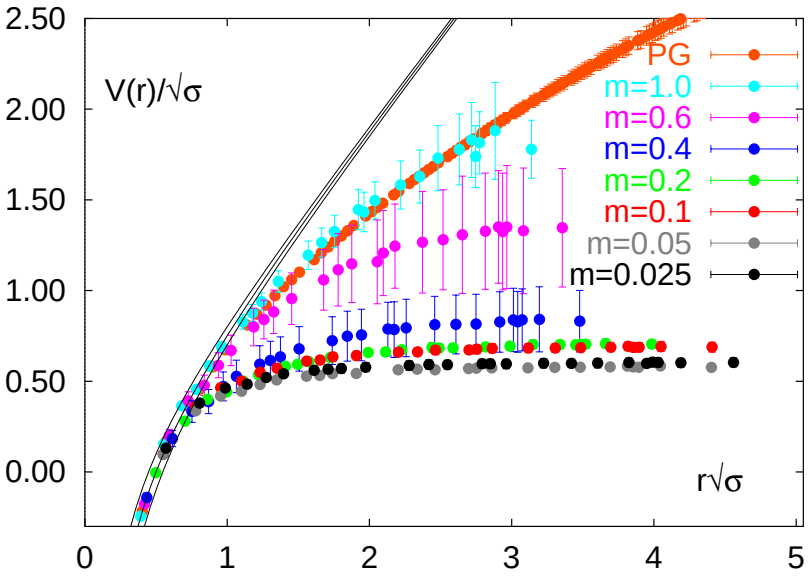

Figure 5: Quark mass dependence of the heavy quark potential for three flavour QCD below the transition temperature at a temperature $T \simeq 0.97\ T_c$. The band of lines gives the Cornell-potential in units of the square root of the string tension, $V(r)/\sqrt{\sigma} = -\alpha/r\sqrt{\sigma} + r\sqrt{\sigma}$ with $\alpha = 0.25 \pm 0.05$.The gauge couplings corresponding to the different quark mass values are $\beta = 4.06$, 3.97, 3.86, 3.76, 3.59, 3.46, 3.38, 3.32 (from top to bottom).

with the same quark mass than to the 3-flavour case. We thus expect that the critical temperature of 2-flavour QCD provides a good approximation to the physically realized case of two light and a heavier strange quark.

4 The heavy quark free energy

We have discussed in the previous sections the influence of dynamical quarks on the QCD transition temperature. In addition to the quark mass dependence of T_c we also expect that the presence of dynamical quarks of finite mass in the thermodynamic heat bath will lead to large qualitative and quantitative modifications of the heavy quark potential[g] $V(r,T)$. In the pure gauge ($m_q \to \infty$) limit the heavy quark potential is strictly confining for all temperatures below T_c. For any finite quark mass value, however, string breaking will occur and the potential will approach a constant value for $r \to \infty$.

[g]We stick here to the commonly used notion of a heavy quark potential, although at non-zero temperature we are actually dealing with the heavy quark free energy [35].

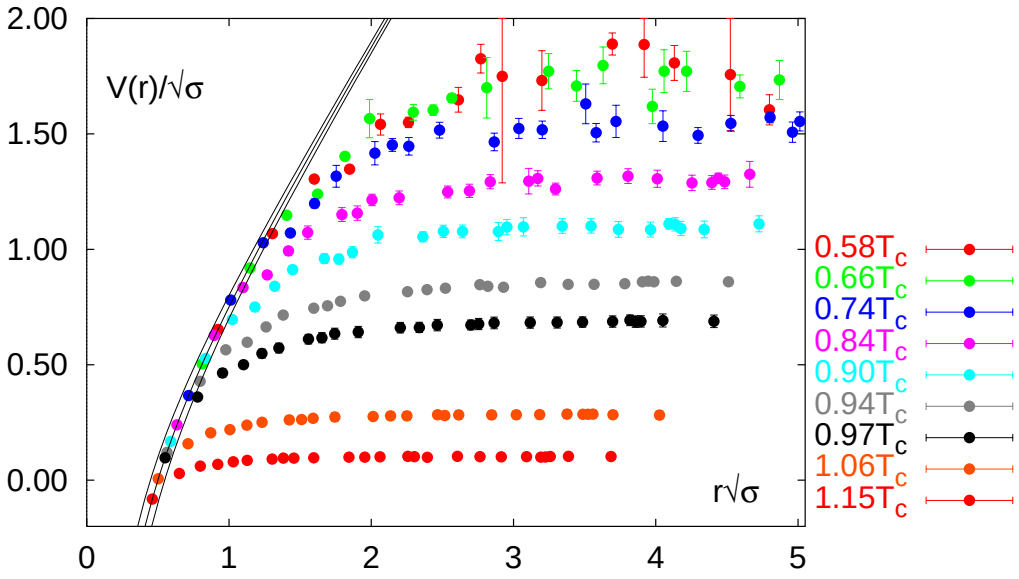

Figure 6: Temperature dependence of the heavy quark potential for three flavour QCD with a quark mass $m_q = 0.1$. The band of lines gives the Cornell-potential in units of the square root of the string tension, $V(r)/\sqrt{\sigma} = -\alpha/r\sqrt{\sigma} + r\sqrt{\sigma}$ with $\alpha = 0.25 \pm 0.05$. The gauge couplings corresponding to the different temperatures are $\beta = 3.25$, 3.30, 3.35, 3.40, 3.43, 3.45, 3.46, 3.50, 3.54. The string tension values used to set the scale are based on the interpolation formula given in Ref. 12. The potentials have been normalized at short distances such that they agree with the zero temperature Cornell potential at $r = 1/4T$.

While it seems to be difficult to detect string breaking in calculations of the heavy quark potential at zero temperature using Wilson loops, string breaking does quite naturally occur at finite temperature, where the heavy quark potential can be extracted from Polyakov loop correlation functions

$$\frac{V_{q\bar{q}}(r,T)}{T} = -\ln\langle L(\vec{x})L^\dagger(\vec{y})\rangle + \text{const.} \quad , \quad \text{with} \quad |\vec{x}-\vec{y}| = r \quad . \tag{4.1}$$

In fact, string breaking is directly related to the non-vanishing of the Polyakov loop expectation value at any temperature and finite quark mass,

$$\lim_{r\to\infty}\left(\frac{V_{q\bar{q}}(r,T)}{T}\right) = -2\ln|\langle L\rangle| + \text{const.} \quad . \tag{4.2}$$

First results on string breaking at finite temperature have been reported in [28].

In order to analyze the quark mass dependence of the heavy quark potential and its structure at large distances we have calculated Polyakov-loop correlation

functions for 3-flavour QCD at a temperature close but below the transition temperature, $T \simeq 0.97\ T_c$. This analysis has been performed with the p4-action on lattices of size $16^3 \times 4$ as a by-product of our determination of the critical couplings at various quark mass values. In addition we used the string tensions obtained from our zero temperature calculations at a nearby value of the gauge coupling, corresponding to $T = T_c$, to set the scale for the potential and the spatial separation r of the static quark anti-quark pair. These potentials are shown in Figure 5. They have been normalized such that they agree with the zero temperature Cornell potential at short distances, *i.e.* at $r = 1/4T$.

We note that with decreasing quark mass the screening effects resulting from the presence of virtual quark anti-quark pairs lead to a more rapid flattening of the potential. While for $m_q = 1.0$ the potential still coincides with the finite temperature potential in the pure gauge sector [36] at least up to $r\sqrt{\sigma} = 3$, the influence of dynamical quarks becomes large already for $m_q = 0.6$. At small quark masses the screened potential reaches a limiting form and starts deviating from the pure gauge heavy quark potential already at $r\sqrt{\sigma} \simeq 0.7$ and saturates at $r\sqrt{\sigma} \simeq 1.5$. This corresponds to distances $r \simeq 0.3$ fm and 0.7 fm, respectively. In general we find that deviations from the chiral limit are small for quark masses below $m_q \simeq 0.1$ or $m_{\rm PS} \simeq 1.8\sqrt{\sigma}$.

The above analysis of the quark mass dependence has been performed at a fixed temperature close to T_c. In addition screening effects are, of course, also strongly temperature dependent. In the pure gauge case this leads to a temperature dependence of the string tension [36]. In the presence of dynamical quarks we find that string breaking sets in at larger distances when the temperature is lowered. Note that this happens although at fixed bare quark mass m_q the physical quark mass decreases with decreasing temperature. Thermal effects seem to become small for temperatures below $T \simeq 0.65\ T_c$. This becomes evident from Figure 6 where we show results from a calculation for 3-flavour QCD with quark mass $m_q = 0.1$. In the low temperature regime the potential starts deviating from simple Cornell-type confinement potential for $r\sqrt{\sigma} \simeq 1.2$ and reaches a plateau for $r\sqrt{\sigma} \simeq 3$. This corresponds to distances $r \simeq 0.6$ fm and 1.4 fm, respectively.

To quantify the screening effect in the presence of light dynamical quarks we define the depth of the potential as the difference between the asymptotic value at large distances and the potential at distance $r\sqrt{\sigma} = 0.5$,

$$\Delta V \equiv \lim_{r\to\infty} V(r) - V(0.5/\sqrt{\sigma}) \tag{4.3}$$

which is the point at which the Cornell-potential vanishes if one chooses the coupling of the Coulomb term as $\alpha = 0.25$. It approximately corresponds to a distance $r \simeq 0.23$ fm. In Figure 7 we show this difference of potential energies.

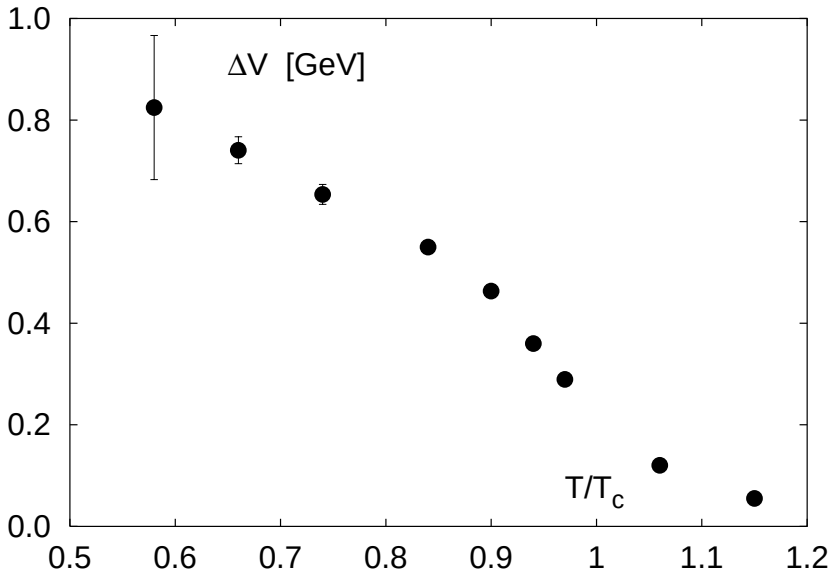

Figure 7: Temperature dependence of the depth of the heavy quark potential, defined in Eq. 4.3, calculated in 3-flavour QCD with quarks of mass $m_q = 0.1$. In order to convert to physical units we have used $\sqrt{\sigma} = 425$ GeV as input.

We note that ΔV changes most rapidly in the vicinity of T_c. At T_c we obtain $\Delta V \simeq 0.5\sqrt{\sigma} \simeq 200$ MeV which, in fact, is compatible with the depth of a simple unscreened Coulomb potential, $V(r)/\sqrt{\sigma} = -\alpha/r\sqrt{\sigma}$ with $\alpha = 0.25$.

5 Conclusions

We have analyzed the quark mass and flavour dependence of the critical temperature of QCD using improved gauge and staggered fermion actions. We find that in a large interval of quark mass values, which corresponds to zero-temperature pseudo-scalar meson masses $m_{\rm PS}$ between 360 MeV and about 2.3 GeV the transition temperature $T_c(m_{\rm PS})$ depends only weakly on $m_{\rm PS}$. In this entire mass interval the transition temperature in two-flavour QCD is about 10% larger than that of three-flavour QCD. An extrapolation of both pseudo-critical temperatures to the chiral limit yields $T_c(0) = (173 \pm 8)$ MeV in the case of two-flavour QCD and $T_c(0) = (154 \pm 8)$ MeV for three-flavour QCD. In both cases we have quoted statistical errors only. From a comparison with calculations performed with unimproved actions and the experience gained with discretization errors in that case as well as in the pure gauge sector we estimate that systematic errors inherent in the present analysis are of the same order of magnitude. The results obtained here with staggered fermions are also consistent with results obtained from studies of two-flavour QCD with clover-improved Wilson

fermions [32].

Our analysis of the temperature and quark mass dependence of the heavy quark free energy shows that screening at $T \simeq 0.97T_c$ is very efficient already in a quark mass regime where the (zero-temperature) pseudo-scalar meson masses are about 1 GeV. Furthermore, screening effects become approximately quark mass independent for smaller masses. For a fixed value of the bare quark mass, $m_q = 0.1$, we find that string breaking effects set in at a distance of about 0.6 fm for small temperatures, $T \lesssim 0.6T_c$. With increasing temperature the onset point gradually shifts to shorter distances. At T_c the heavy quark free energy gets screened already at distances of about 0.3 fm.

Acknowledgements:

The work has been supported by the TMR network ERBFMRX-CT-970122 and by the DFG under grant Ka 1198/4-1.

References

[1] R.D. Pisarski and F. Wilczek, Phys. Rev. D29 (1984) 338.

[2] B. Svetitsky and L.G. Yaffe, Phys. Rev. D26 (1982) 963 and Nucl. Phys. B210 [FS6] (1982) 423.

[3] R.V. Gavai, J. Potvin and S. Sanielevici, Phys. Rev. Lett. 58 (1987) 2519.

[4] see for instance, E. Laermann, Nucl. Phys. B (Proc. Suppl.) 63 (1998) 114.

[5] see for instance: F. Karsch, Nucl. Phys. B (Proc. Suppl.) 83-84 (2000) 14.

[6] H. Meyer-Ortmanns and B.-J. Schaefer, Phys. Rev. D53 (1996) 6586.
J. Berges, D.-U. Jungnickel and C. Wetterich, Phys. Rev. D59 (1999) 034010.

[7] R. Hagedorn, Nuovo Cimento Suppl. 3 (1965) 147.

[8] M.J. Teper, *Glueball masses and other physical properties of SU(N) gauge theories in D=3+1: A review of lattice results for theorists*, hep-th/9812187.

[9] R. D. Pisarski and O. Alvarez, Phys. Rev. D26 (1982) 3735.

[10] B. Beinlich, F. Karsch, E. Laermann and A. Peikert, Eur. Phys. J. C6 (1999) 133.

[11] U.M. Heller, F. Karsch and B. Sturm, Phys. Rev. D60 (1999) 114502.

[12] F. Karsch, E. Laermann and A. Peikert, Phys. Lett. B478 (2000) 447.

[13] T. Blum, C. De Tar, S. Gottlieb, K. Rummukainen, U.H. Heller, J.E. Hetrick, D. Toussaint, R.L. Sugar and M. Wingate, Phys. Rev. D55 (1997) 1133.

[14] S. Gottlieb, W. Liu, D. Toussaint, R.L. Renken and R.L. Sugar, Phys. Rev. D35 (1987) 2531.

[15] S. Aoki et al. (JLQCD), Phys. Rev. D57 (1998) 3910.

[16] A.M. Ferrenberg and R.H. Swendsen, Phys. Rev. Lett. 61 (1988) 2635.

[17] S. Fortunato and H. Satz, Phys. Lett. B475 (2000) 311.

[18] P. Hasenfratz, F. Karsch and I.O. Stamatescu, Phys. Lett. 133B (1983) 221.

[19] S. Aoki et al. (JLQCD), Nucl. Phys. B (Proc. Suppl.) 73 (1999) 459.

[20] M. Lütgemeier, *Phasenübergänge in der QCD mit fundamentalen und adjungierten Quarks*, Ph.D. thesis, Bielefeld 1998.

[21] S. Gottlieb et al., Phys. Rev. D35 (1987) 3972.

[22] M. Fukugita, H. Mino, M. Okawa and A. Ukawa, Phys. Rev. D42 (1990) 2936.

[23] F. Karsch and E. Laermann, Phys. Rev. D50 (1994) 6954.

[24] A. Gonzalez Arroyo, F.J. Yndurain and G. Martinelli, Phys. Lett. 117B (1982) 437; erratum Phys. Lett. B122 (1983) 486.

[25] R. Altmeyer et al., Nucl. Phys. B389 (1993) 445.

[26] M. Albanese et al., Phys. Lett. B192 (1987) 163.

[27] C. Bernard et al., *Zero Temperature String Breaking with Staggered Quarks*, hep-lat/0010066 and references therein.

[28] C. DeTar, O. Kaczmarek, F. Karsch and E. Laermann, Phys. Rev. D59 (1999) 03150.

[29] S. Aoki et al. (CP-PACS Collaboration), Phys. Rev. Lett. 84 (2000) 238.

[30] H. Wittig, Int. J. Mod. Phys. A12 (1997) 4477.

[31] for a recent discussion see: G. Bali, *QCD forces and heavy quark bound states*, hep-ph/0001312.

[32] A. Ali Khan et al. (CP-PACS Collaboration), *Phase structure and critical temperature of two flavor QCD with renormalization group improved gauge and clover improved Wilson quark action*, hep-lat/0008011.

[33] M. Okamoto *et al.* [CP-PACS Collaboration], Phys. Rev. D60 (1999) 094510.

[34] C. Bernard *et al.*, Phys. Rev. D54 (1996) 4585 and references therein.

[35] L.D. McLerran and B. Svetitsky, Phys. Lett. B98 (1981) 195.

[36] O. Kaczmarek, F. Karsch, E. Laermann and M. Lütgemeier, Phys. Rev. D62 (2000) 034021.